Comparative study of atmospheric pressure low and radio frequency microjet plasmas produced in a single electrode configuration

Dan Bee Kim, J. K. Rhee, B. Gweon, S. Y. Moon, and W. Choe[a)]
Department of Physics, Korea Advanced Institute of Science and Technology, 335 Gwahangno, Yuseong-gu, Daejeon 305-701, Korea

(Received 16 July 2007; accepted 17 September 2007; published online 11 October 2007)

Microsize jet-type plasmas were generated in a single pin electrode structure source for two separate input frequencies of 50 kHz and 13.56 MHz in the ambient air. The copper pin electrode radius was 360 μm, and it was placed in a Pyrex tube with a radius of 3 mm for helium gas supply. Due to the input frequency difference, the generated plasmas showed distinct discharge characteristics for their plasma physical appearances, electrical properties, gas temperatures, and optical properties. Strengths and weaknesses of both plasmas were discussed for further applications. © *2007 American Institute of Physics*. [DOI: 10.1063/1.2794774]

Nonthermal atmospheric pressure plasmas have gathered great interest for their favorable properties and potentials in applications. For instance, they do not require an expensive high vacuum system, but they contain enough radicals for effective treatments of materials and still have gas temperature low enough not to harm the materials.[1] Yet, there is a problem in generating a uniform nonthermal atmospheric pressure plasma with a large volume compared to the low pressure cases. Thus, small size nonthermal atmospheric pressure plasmas are recently focused on to overcome the problem and meet the demand for small size applications. Compared to the large size atmospheric pressure plasmas, small size plasmas tend to be stable and generate many chemically reactive radicals with high energy electrons.[2] As a result, the small size plasmas have been generated in various types and applied to many fields, especially the bio/medical fields.[3]

The nonthermal atmospheric pressure plasma sources can be divided according to the input frequency in one way. One of the representative sources is the dielectric barrier discharge (DBD) plasmas, which typically employ low frequency (LF) of several tens of kilohertz.[4] Especially, plasmas generated in a pin to dielectric barrier plane electrode structure or referred to as corona-DBD hybrid plasmas are frequently investigated for small size plasma generations using LF.[5] Meanwhile, radio frequency (rf) of 13.56 MHz is widely employed in planar or coaxial cylindrical capacitively coupled plasma (CCP) sources. Recently, the rf coaxial cylindrical CCP source is chosen to generate small size jet-type plasmas.[6] Small size plasmas are usually generated in the jet type for both LF and rf. Since it is in the early stage of study, both LF and rf small size nonthermal atmospheric pressure plasmas have been independently investigated, each originated from different plasma sources. However, as they evolve, their sources end up in a similar structure of the pin electrode. Therefore, for now, it is needed to study each in more detail and compare their discharge characteristics in order to define their distinct features and to clarify advantages and disadvantages of each. Furthermore, even both can be combined to generate the dual frequency small size nonthermal plasma exhibiting advantages of both plasmas.

In this work, first, a plasma source of single pin electrode configuration was fabricated and powered by either LF or rf with the helium gas supply to generate a microsize jet-type plasma in the same source configuration except using the different driving power sources. Then, after the plasma production, their discharge characteristics, such as physical appearance, electrical properties, gas temperature, and emission spectrum, were investigated for further analysis and comparison.

The plasma source consists of a copper pin of a radius of 360 μm. The copper pin electrode, except for the pin head, was covered by a dielectric material for the focused plasma generation at the head, and it was placed in a Pyrex tube of 3 mm in radius for the helium gas supply. The pin electrode was powered by either a LF power source (FTLab HPSI200) or a rf power source (YS E06F) through a matching network. The LF power source was fixed at 50 kHz, and the rf power source frequency was 13.56 MHz. Plasmas were generated in the ambient air.

To reduce the experimental parameters, the helium gas flow rate was fixed at 3 l/m. The variation of the gas flow rate affected the LF plasma much more than the rf plasma. For most circumstances, the electrode head was fixed at 5 mm inside from the Pyrex tube end. The breakdown voltage decrease was observed for both LF and rf when the pin electrode was placed deeper in the Pyrex tube. Furthermore, both plasmas were studied with a target, bearing in mind the applications.[5] The detailed results of the parametric and application feasibility studies will be presented elsewhere.

The LF plasma image is shown in Fig. 1(a) for three different pin electrode positions. The longer plasma length was observed when the electrode was placed deeper in the Pyrex tube. The LF plasma has a long cylindrical shape, and its length from the electrode varied between 5 and 30 mm for the increasing discharge voltage, as illustrated in Fig. 1(b). The abrupt decrease of the plasma length at around 1300 V is due to the change in the plasma. At low voltages, the plasma was rather thick in radius, and as the voltage was increased, the plasma volume grew in the axial direction with a bright core region appearing in the center. Then, at a certain voltage (V_{in}=1300 V), only the bright thin core region was remained, and this causes the abrupt drop of the

[a)]Author to whom correspondence should be addressed. Electronic mail: wchoe@kaist.ac.kr

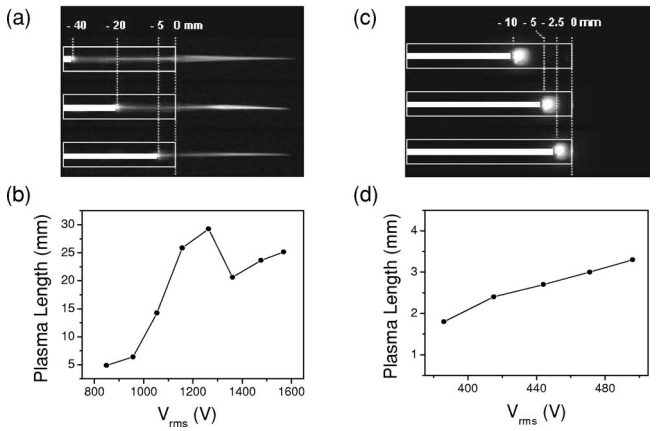

FIG. 1. (a) LF and (c) rf plasma images for three different electrode positions. (b) LF and (d) rf plasma length variations when the electrode was 5 mm inside from the Pyrex tube end.

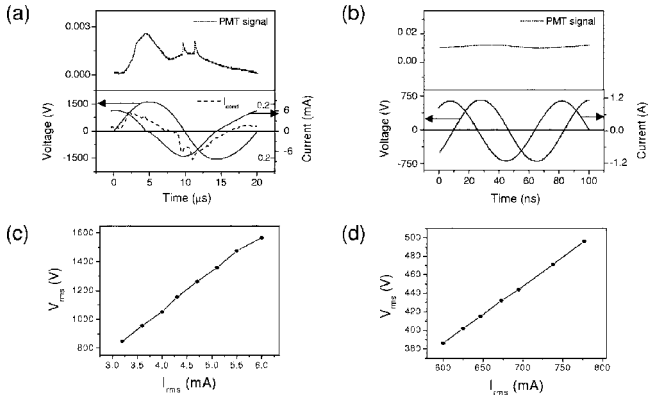

FIG. 2. Voltage and current waveforms and plasma light emission signal for (a) LF plasma at $V_{in}=1100$ V (dashed curve in the lower graph represents the conduction current waveform) and (b) rf plasma at $P_{in}=100$ W. Total current vs voltage curves for (c) LF and (d) rf plasmas.

plasma length. On the other hand, the rf plasma was more or less of spherical shape [Fig. 1(c)], and its length did not increase much for the varying electrode position nor the discharge voltage, as shown in Fig. 1(d).

The physical difference of the LF and rf plasmas was attributed to the input frequency difference as the electron displacement is a function of the input frequency. In an external oscillating electric field of $E=E_a \sin \omega t$, the electron oscillatory displacement r can be approximated to

$$r = \frac{eE_a}{m_e \omega \sqrt{\omega^2 + \nu_m^2}} \sin(\omega t + \phi), \tag{1}$$

where $\omega=2\pi f$ is the oscillation frequency of the external electric field, ν_m is the effective collision frequency of electron, and $\phi=\tan^{-1}(\nu_m/\omega)$. In the limiting case of very frequent collisions ($\nu_m \gg \omega$), as in the atmospheric pressure plasma, Eq. (1) simplifies to

$$r = \frac{eE_a}{m_e \omega \nu_m} \cos \omega t = \frac{\mu_e E_a}{\omega} \cos \omega t, \tag{2}$$

where μ_e is the electron mobility. In such collisional condition, the electrons follow a relatively slow field evolution as if they were in a dc field.[7] As can be clearly seen from Eq. (2), electrons oscillate with larger amplitudes for lower frequency. In other words, the electrons are less locally confined near the electrode for the lower frequency. Since it is mainly the electrons that play an important role in the plasma ionization process, the electron oscillatory displacement is related to the plasma physical size.

In order to support the above argument, the maximum electron displacement r_{max} $(=\mu_e E_a/\omega)$ was roughly estimated using μ_e given in Ref. 8. The electric field was calculated based on the measured discharge voltage using a simple geometry of pin to plane with the plane at a remote distance. As a result, r_{max} was estimated to be 500–1000 mm for LF and 6–13 mm for rf. Such results might be larger than actual numbers, because μ_e depends on pressure and electric field strength. Nevertheless, the estimated r_{max} meets the measured plasma length for the rf case. For the LF case, on the other hand, the estimated r_{max} is about an order larger than the measured plasma length. However, in our experiments, as already mentioned, the plasma length kept increasing as the pin electrode was placed deeper inside the Pyrex tube. The similar plasma lengths from the tube end for different electrode positions infer that the short plasma length is due to the decrease in the helium gas purity outside the tube with the air impurity. As a matter of fact, it was reported that the atmospheric pressure argon plasma generated at 20 kHz with a typical injection needle placed in a Teflon tube was as long as 1000 mm.[9]

The current and voltage were measured using a current probe (Pearson 4100) and a voltage probe (Tektronix P6015A), and wavelength-unresolved visible emission from the plasma was measured using a photomultiplier tube (Hamamatsu R928-10). Figure 2(a) depicts waveforms of input voltage, total current, and optical emission signal of the LF plasma. Although the total current does not clearly show the peaks, the conduction current, obtained by subtracting the displacement current from the total current and drawn with the dashed curve, has peaks corresponding to the emission signal as the peaks correspond to each other. Similar waveforms are illustrated in Fig. 2(b) for the rf plasma. Both the current waveform and the emission signal imply that the discharge is rather continuous compared with the LF discharge. Again, such dissimilarity in the discharge characteristics is attributed to the input frequency difference. At 50 kHz, both electrons and ions follow the electric field, but at 13.56 MHz, only electrons of much higher mobility follow the field while ions only experience the average field.[1] Then, for the rf plasma, it is always with the electrons that density profile instantaneously changes with the field, resulting in a rather continuous and symmetric discharge.[10] However, for the LF plasma, both electrons and ions move along the field, and due to their mobility difference, asymmetry was observed in the current waveform and emission signal.[11]

Also, discharge voltage and current are represented in Fig. 2(c) for the LF plasma and Fig. 2(d) for the rf plasma. The discharge voltage was higher for the LF plasma than the rf plasma. At LF, the oscillation amplitude is larger, and both electrons and ions respond to the field and are able to reach the source boundary, i.e., the pin electrode in this case and/or the target material if it is present. As a result, both species are largely lost by hitting the boundary, and the plasma is rather sustained by secondary electrons. For the higher frequency, the secondary electron production is reduced and the breakdown voltage is increased since ions start to fail in following the field. However, as the frequency is increased further above a few megahertz, since only the electrons follow the

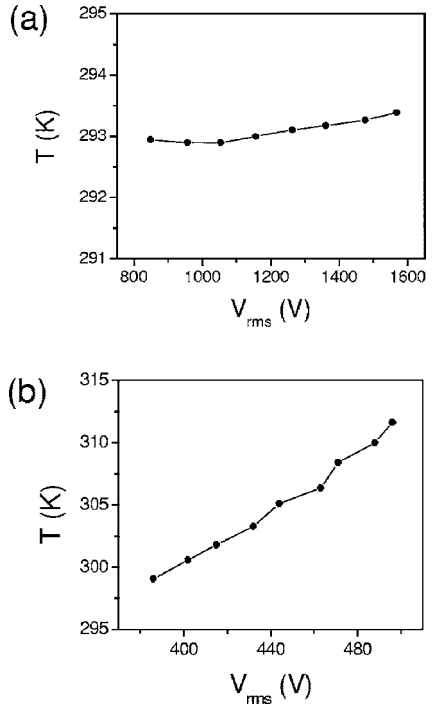

FIG. 3. Plasma gas temperature plots for (a) LF and (b) rf plasmas.

field, the electron loss and the breakdown voltage are largely reduced due to the great reduction in the oscillation amplitude.[12] Therefore, the breakdown and discharge voltages of the rf plasma are much lower than those of the LF plasma. Furthermore, the power dissipated to the plasma, $P_{\mathrm{diss}}=1/T\int_0^T VIdt$, was in the range of 110–370 mW for the LF and 20–30 W for the rf.

The gas temperature was measured using a fiber thermometer (FISO FOT-H). The validity of the fiber thermometer was confirmed by comparing the temperature values with those from the optical emission spectroscopy based on the N_2^+ (391.4 nm) spectra.[13] From Fig. 3(a), it is seen that the LF gas temperature was only a little higher than the room temperature (292 K) and stayed about the same when varying the discharge voltage. Besides, as shown in Fig. 3(b), the rf gas temperature was started from the room temperature and increased up to about 310 K as the discharge voltage was increased.

Shown in Fig. 4 are the plasma emission spectra obtained by a visible spectrometer (Chromex 250is). The upper graph representing the LF plasma emission spectrum shows that there were nitrogen molecular lines as well as a few helium and oxygen atomic lines. The lower graph of Fig. 4 illustrates the rf plasma emission spectrum with nitrogen molecular lines and a larger number of helium and oxygen atomic lines of much higher intensities than the LF plasma. More He I lines, especially in the short wavelength range, indicates the higher degree of ionization for the rf plasma, and the N_2^+ line is related to He^* and He_2^+ concentrations.[14,15] Therefore, it can be inferred from the emission spectra that the rf plasma density and/or electron temperature is much higher.

In conclusion, microsize jet-type plasmas were generated in a single pin electrode structure for two input frequencies of 50 kHz and 13.56 MHz, and they showed several distinct discharge characteristics. First, the LF plasma was

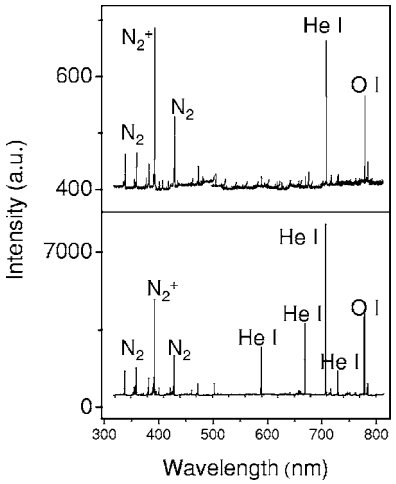

FIG. 4. Plasma emission spectrum of LF plasma (upper) at $V_{\mathrm{in}}=1100$ V and rf plasma (lower) at $P_{\mathrm{in}}=100$ W.

about ten times longer than the rf plasma. The larger plasma length can be advantageous for treating objects as too short distance between the plasma source and the object can become a source of inconvenience or spark generation. Second, the discharge characteristics were more continuous in time in the case of the rf plasma as seen from the current and plasma emission measurements. The continuity in the waveform is somehow related to the plasma homogeneity; thus, the rf plasma may be more favorable for its better homogeneity. Third, the LF gas temperature was as low as the room temperature. The temperature tends to increase in the presence of a target, thus, the LF plasma is preferred over the rf plasma when it comes to the temperature. Finally, the plasma emission spectrum of the rf plasma had much higher intensity and more helium atomic emission lines indicating larger plasma density and/or electron temperature.

This work was supported by the Defense Acquisition Program Administration and Agency for Defense Development under Contract No. UD060005AD.

[1] C. Tendero, C. Tixier, P. Tristant, J. Desmaison, and P. Leprince, Spectrochim. Acta, Part B **61**, 2 (2006).
[2] K. H. Becker, K. H. Schoenbach, and J. G. Eden, J. Phys. D **39**, R55 (2006).
[3] E. Stoffels, A. J. Flikweert, W. W. Stoffels, and G. M. W. Kroesen, Plasma Sources Sci. Technol. **11**, 383 (2002).
[4] U. Kogelschatz, Plasma Chem. Plasma Process. **23**, 1 (2003).
[5] D. B. Kim, J. K. Rhee, S. Y. Moon, and W. Choe, Appl. Phys. Lett. **89**, 061502 (2006).
[6] Schütze, J. Y. Jeong, S. E. Babayan, J. Park, G. S. Selwyn, and R. F. Hicks, IEEE Trans. Plasma Sci. **26**, 6 (1998).
[7] Y. P. Raizer, M. N. Shneider, and N. A. Yatsenko, *Radio-Freqeuncy Capacitive Discharges* (CRC, Boca Raton, FL, 1995), p. 3.
[8] Y. P. Raizer, *Gas Discharge Physics* (Springer, Moscow, 1987), p. 11.
[9] Y. C. Hong, S. C. Cho, J. H. Kim, and H. S. Uhm, Phys. Plasmas **14**, 074502 (2007).
[10] Y. Sakiyama and D. B. Graves, J. Phys. D **39**, 3451 (2006).
[11] H. Ueno, K. Hata, and H. Nakayama, Jpn. J. Appl. Phys., Part 1 **46**, 1142 (2007).
[12] M. Radmiloviæ-Radjenoviæ and J. K. Lee, Phys. Plasmas **12**, 063501 (2005).
[13] S. Y. Moon and W. Choe, Spectrochim. Acta, Part B **58**, 249 (2003).
[14] N. K. Bibinov, A. A. Fateev, and K. Wiesemann, Plasma Sources Sci. Technol. **10**, 579 (2001).
[15] J. M. Pouvesle, A. Bouchoule, and J. Stevefelt, J. Chem. Phys. **77**, 817 (1982).